ACS OMEGA

Open Access

http://pubs.acs.org/journal/acsodf

Article

Effect of Particle Size and Hydrophobicity on Bubble-Particle Collision Detachment at the Slurry−Foam Phase Interface

Yiqing Zhang,[§] Shihao Ding,[§] Weihan Si, Qinglin Yin, Chenyimin Yang, Wenqing Shi, Yaowen Xing,* and Xiahui Gui

Cite This: *ACS Omega* 2024, 9, 4966−4973

Read Online

ACCESS | Metrics & More | Article Recommendations

ABSTRACT: The slurry phase, foam phase, and slurry−foam phase interfaces are the typical locations for bubble-particle detachment, and significant advancements have been achieved in the detachment theory of the slurry phase and foam phase. However, the microscopic detachment mechanism of particles at the slurry−foam phase interface is still unclear. Specifically, there is still debate concerning the collision detachment mechanism of bubble-particle aggregates. Thus, this work investigated the effects of particle size and hydrophobicity on bubble-particle collision detachment. First, a tensiometer detected the detachment force between particles and bubbles. Next, using a high-speed dynamic camera, the collision detachment probability and detachment behavior of bubble-particle aggregates at the interface (solid surface) were statistically recorded and captured. Last, MATLAB software was used to analyze the trajectory and velocity of the particles and the velocity and projected area of the bubbles in the process of bubble-particle collision detachment. This allows for a deeper investigation of the mechanism underlying the detachment of particles of various sizes and hydrophobicity. It is discovered that as particle hydrophobicity increases, the probability of bubble-particle collision detachment reduces. This is because when particle hydrophobicity increases, so does the interaction force between particles and bubbles, improving the stability of the bubble-particle aggregates. Simultaneously, it is discovered that there are notable differences in the collision detachment mechanisms of various particle sizes. Due to their low gravity, the fine particles in the bubble-particle aggregate will slide down the bubble's surface when it collides with the solid surface. This differential velocity motion between the particle and the bubble plays a significant role in the fine particles' detachment. However, the gravity of the coarse particles is strong enough to squeeze the bubbles vertically, and bubble oscillation is an important reason for the detachment of the bubble-particle aggregates. The study's findings advance our understanding of the bubble-particle collision detachment mechanism and offer a theoretical direction for investigating collision detachment behavior at the real slurry−foam phase interface.

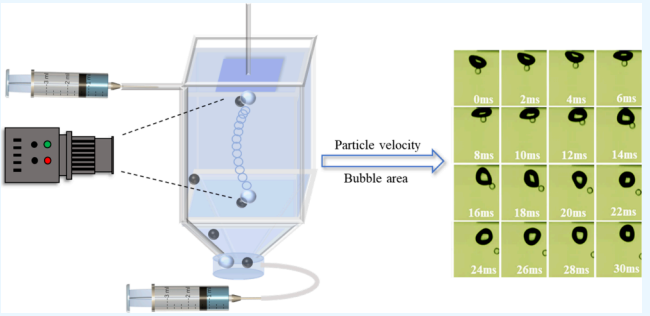

1. INTRODUCTION

Flotation is an interface separation technique that selectively separates valuable minerals from gangue minerals by taking advantage of the variations in the physical and chemical characteristics of particle surfaces.[1,2] The three subprocesses of bubble particle mineralization—collision, attachment, and flotation of bubble-particle aggregates—make up the fundamental component of flotation.[3−5] The ultimate flotation efficiency and maximum size of a particle that may float are determined by the detachment behavior of the particles.

The examination of bubble-particle aggregate force balance, which is where the classic research on bubble-particle detachment begins, favors the turbulent centrifugal detachment hypothesis.[6−8] The detachment of spherical particles stuck to bubbles was investigated by Nutt.[9] The particles were extracted from the gas−liquid interface utilizing an external flow field's centrifugal force. To determine the critical detachment force of particles, a theoretical calculation model for centrifugal, buoyancy, and capillary forces was developed. By taking into account the effect of turbulent vortices on bubble-particle detachment, Schulze et al.[10,11] substantially improved this theory. The particle will separate from the bubble surface when the centrifugal force is greater than the force between particles and bubbles.

Bubble-particle detachment occurs primarily at the foam and slurry−foam interfaces, as well as in the slurry phase.[12,13] Ata[14] used an experimental system to investigate how bubble

Received: November 9, 2023
Revised: December 11, 2023
Accepted: December 28, 2023
Published: January 18, 2024

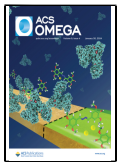

merging affects bubble-particle detachment behavior. The findings indicate that the bubble merger will result in bubble oscillation and a decrease in bubble surface area, which will impair the bubble surface's payload capacity and trigger bubble-particle detachment.[15] Furthermore, Ata[14] discovered that there was a functional relationship between the bubble merging time and the particle coverage on the bubble surface that was monotonically increasing. In other words, the longer the bubble merging time, the higher the particle coverage on the bubble surface, suggesting that the particles attached to the bubble surface would have some damping effect on bubble merging. The slurry−foam phase interface and bubble-particle detachment process have complex features; the detachment mechanism is unknown. According to some researchers, the primary cause of bubble-particle detachment is the change in kinetic energy that occurs when the bubble-particle aggregate impinges on the interface. According to Falustu and Dobby,[16,17] a significant amount of bubble-particle aggregates were detached at the slurry−foam phase interface. This was thought to be caused by a shift in kinetic energy that occurred both before and after the bubble-particle aggregates collided. According to Seaman et al,[18] bubble-particle detachment was produced by the change in kinetic energy brought about by the aggregate traveling across the slurry−foam phase interface as well as bubble oscillation. Selective detachment was seen as a result of the distinct characteristics of the particles. Other researchers, on the other hand, have discovered that bubble-particle detachment in this region is primarily caused by the bubble merger and the disturbance brought about by the interface region rather than the change in kinetic energy at the slurry−foam phase interface.[19] A high-speed dynamic camera was employed by Irelan and Jameson[20] utilizing a test apparatus to monitor the movement and collision of the bubble-particle aggregates at the interface. The findings demonstrate that the majority of the particles remain attached to the bubble even after collision, suggesting that the bubble-particle aggregates' kinetic energy was dispersed during the initial stages of collision with the interface. As a result, the particles only move smoothly on the bubble's surface and retain their attachment state. There is ongoing debate about the collision detachment mechanism of the bubble-particle aggregates at the slurry−foam phase interface.

This study investigates the impact of particle size and hydrophobicity on the detachment behavior of bubble-particle aggregates at the solid interface.[21] Using a tensiometer, the detachment force between particles and bubbles was determined. The collision detachment probability and detachment behavior of the bubble-particle aggregates at the solid surface were statistically recorded by using a high-speed dynamic camera. Last, the mechanism of bubble-particle collision detachment with varying hydrophobicity and sizes was investigated by analyzing particle trajectory and velocity, bubble velocity, and projected area by using MATLAB software. A thorough comprehension of the phase interface collision detachment mechanism is essential for enhancing the flotation process's bubble-particle detachment mechanism and serving as a roadmap for increasing the maximum flotation particle size.[22]

2. EXPERIMENTAL SECTION

2.1. Materials. The glass beads employed in this experiment have diameters of 0.5 and 1 mm, respectively, and have consistent characteristics and smooth surfaces. The glass beads' surface was cleaned using acetone, ethanol, and ultrapure water before modification. The cleaned particles were added to varying quantities of a dodecylamine hydrochloride (DAH) solution to alter the hydrophobicity of the glass beads. To guarantee that the particle was consistently hydrophobic, a magnetic stirrer was employed for 30 min. The suspension method was used to measure the modified glass beads' contact angle. Three distinct contact angles were hydrophobic for 0.5 mm glass beads: 55°, 60°, and 65°; three different contact angles were hydrophobic for 1 mm glass beads: 60°, 65°, and 70°.

2.2. Bubble-Particle Interaction Force Test. The JK99M2 tensiometer is used to measure the interaction force between the bubble and the particle, and it is capable of measuring the attachment and detachment forces between bubbles and particles on a microscale. As illustrated in Figure 1, a bubble-particle interaction force measurement system

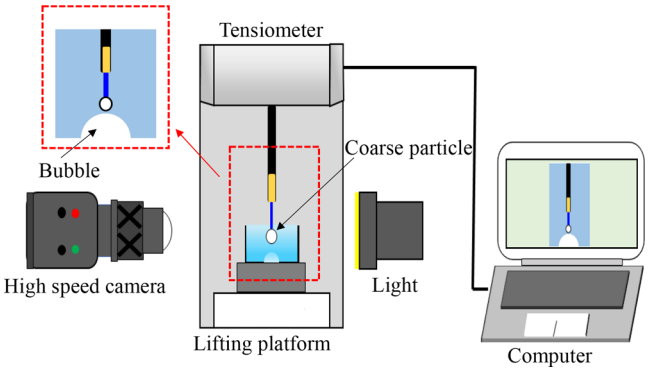

Figure 1. Bubble-particle interaction force measurement system.

consists of a camera, light, glass cell, lifting platform, tensiometer, and computer. It mainly measures the interaction force between particles and bubbles through an internal analytical balance. With a contact angle of 150°, a bubble through superhydrophobic glass sheets fixes the sample tank's bottom.

Before the test began, a microsyringe was used to create a bubble with a diameter of about 2.5 mm on the superhydrophobic glass sheet at the bottom of the sample tank. A capillary tube containing particles was secured to the gripper device of the tensiometer. The lifting platform is driven by the computer to move upward at a speed of 0.01 mm/s, causing particles and bubbles to contact and adhere, and then downward until the particles and bubbles are entirely separated, allowing the computer to process and output the test data.

2.3. Observation of Bubble-Particle Collision Detachment Behavior. As illustrated in Figure 2, a bubble-particle collision detachment behavior observation system consists of a high-speed dynamic camera, an observation tank, a light, a syringe, a capillary, a collision substrate, a manual displacement platform, and a computer. The bottom of the tank is constructed as a pyramid-shaped tank, and a cylindrical groove is created to allow particles to separate from the bubble surface and return to a fixed place, facilitating the subsequent collision test. The side wall of the sink is fixed with a capillary tube connecting a cylindrical groove, and the other end of the capillary tube is connected to a syringe to produce bubbles and particles for collision and attachment. To increase the probability that particles and bubbles will collide at the

https://doi.org/10.1021/acsomega.3c08918
ACS Omega 2024, 9, 4966−4973

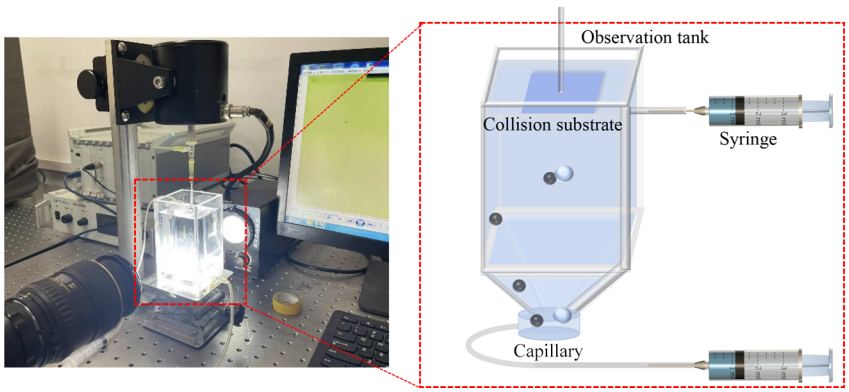

Figure 2. Bubble-particle collision detachment behavior observation system.

capillary port and produce an ascending bubble-particle aggregate, a syringe is positioned horizontally in the bottom groove and filled with the solution. As a collision substrate for bubble-particle aggregates, a fixed device horizontally fixes a sapphire (Al_2O_3) substrate to prevent the bubble-particle aggregate from adhering to the substrate during the collision. The sample sapphire sheet has a side length of 2.5 cm and a thickness of 0.2 mm.

The test observation tank is filled with the hydrophobic glass beads and solution, and the collision substrate is raised to the desired liquid level height. A 3.0 mm bubble is created at one end of the capillary tube using the syringe under control. The horizontal syringe is adjusted at the same time to cause the glass beads in the groove to migrate in the direction of the bubble and crash with it to create a bubble-particle aggregate. The bubble-particle aggregate floats upward from the bottom of the groove due to buoyancy until it collides with the substrate. A high-speed dynamic camera recorded the bubble-particle detachment behavior during this collision.

2.4. Image Processing. Matlab software was used to monitor the motion trajectory of particles and bubbles and to examine the motion state to further explore the collision detachment behavior of bubble-particle aggregates. From the trajectory of the particles, the position coordinate data are collected. It investigated how the velocity of particles changed during ascent, collision, and separation. The motion path of the bubble-particle aggregates generated by two particles of different sizes is shown in Figure 3. In the slurry phase, the bubble-particle aggregate does not rise vertically but swings left and right instead. The trajectory is an "S" curve, and the particles have been sliding on the surface of the bubble.

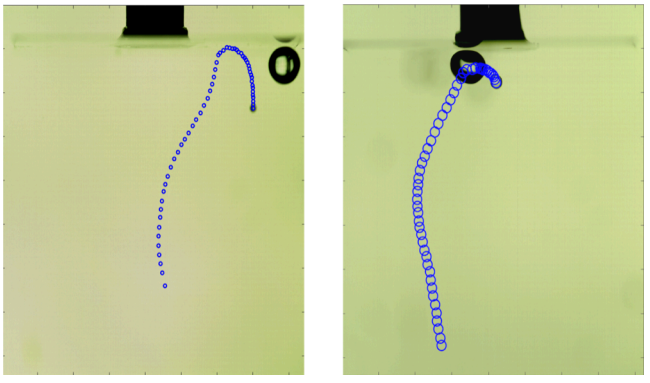

Figure 3. Movement trajectory of particles with different sizes: (a) 0.5 mm particle and (b) 1 mm particle.

3. RESULTS AND DISCUSSION

3.1. Bubble-Particle Interaction Force Test. To clarify the effect of particle hydrophobicity on the interaction force between particles and bubbles, smooth glass beads with a diameter of 0.5 mm and contact angles of 55°, 60°, and 65° were selected to test the detachment force between different hydrophobic particles and bubbles in the tensiometer. The test results are shown in Figure 4. The detachment force between

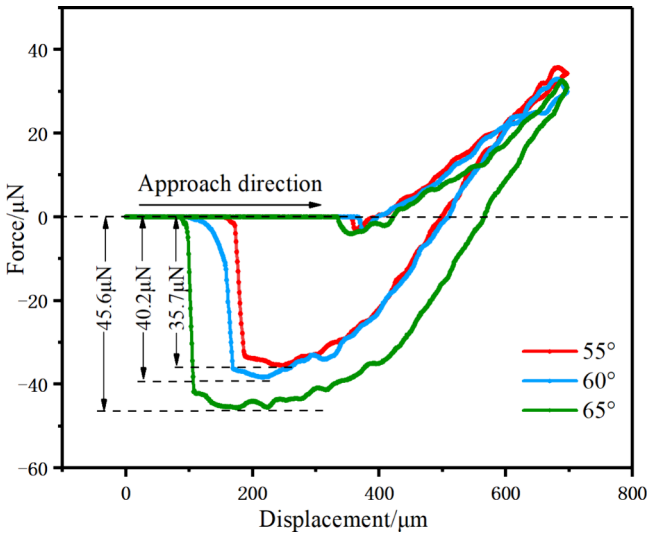

Figure 4. Change curves of interaction force in the process of bubble-particle detachment with 0.5 mm particles under different hydrophobicity.

particles and bubbles increased progressively with a rise in particle hydrophobicity, reaching values of 35.7, 40.2, and 45.6 μN, in that order. This is mostly due to the particles being more hydrophobic, which lengthens the three-phase contact line between particles and bubbles.[23,24]

For the bubble-particle interaction force testing, glass beads with a diameter of 1 mm and contact angles of 60°, 65°, and 70° were chosen. By comparing the test results of 0.5 mm particles with the same contact angle, we investigated the effect of the particle size on the detachment force and stability of the bubble-particle aggregate. The interaction force change curves of 1 mm glass beads during the bubble-particle detachment

https://doi.org/10.1021/acsomega.3c08918
ACS Omega 2024, 9, 4966−4973

process are depicted in Figure 5. The critical detachment force of 1.0 mm particles is 51.6 56.1, and 65.8 μN, 56.1 μN and

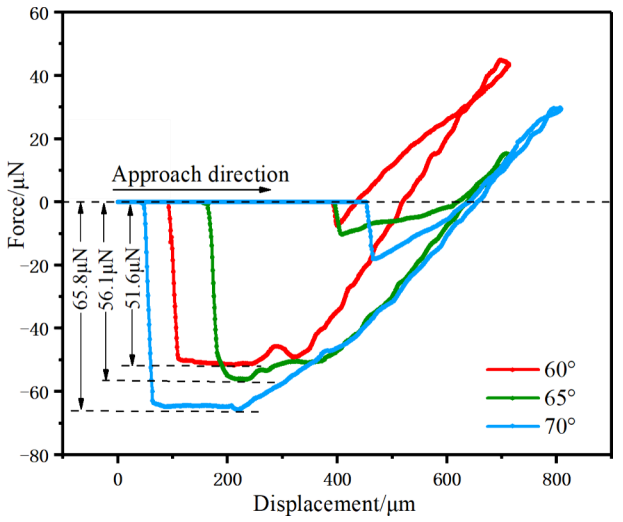

Figure 5. Change curves of interaction force in the process of bubble-particle detachment with 1 mm particles under different hydrophobicity.

65.8 μN, respectively. Both values are higher than 0.5 mm particles under the same hydrophobicity. This is mostly because as the particle size grows, so does the force needed to initiate detachment between particles and bubbles. The detachment force, on the other hand, is proportional to the particle mass or, more specifically, proportionate to the cube of the particle size according to the force analysis of the particle detachment process. Coarse particles detach more readily than fine particles because the attachment is simply proportional to the particle size.[25,26]

The process of flotation is dynamic and ongoing, and the bubble-particle aggregate is vulnerable to a variety of unsettling circumstances.[27] As a result, it is impossible to assess the difficulty of mineral particle flotation solely by measuring the interaction force between quasi-static particles and bubbles. To examine the factors affecting particle detachment, further research on the dynamic detachment process of bubble-particle aggregates is required.

3.2. Probability Test of Bubble-Particle Collision Detachment. Using a high-speed dynamic camera, we examined the collision detachment probability of the bubble-particle aggregates at the slurry−foam interface (solid surface). For the collision detachment test, three different types of hydrophobic glass beads with diameters of 0.5 and 1 mm were chosen, and the collision probability under various particle sizes and hydrophobicity was examined. Figure 6 illustrates the results of the 50 tests that each group performed to determine the collision detachment probability under various circumstances. When the particle size is the same, the collision detachment probability decreases as the hydrophobicity increases. Additionally, an increase in hydrophobicity can greatly strengthen the attachment between the particle and the bubble, improve the stability of the bubble-particle aggregates, and lower the collision detachment probability. When 0.5 and 1 mm particles with the same hydrophobicity were investigated for collision detachment behavior, the bubble-coarse particle aggregates showed a larger detachment probability. The attachment between the particle and the bubble can increase

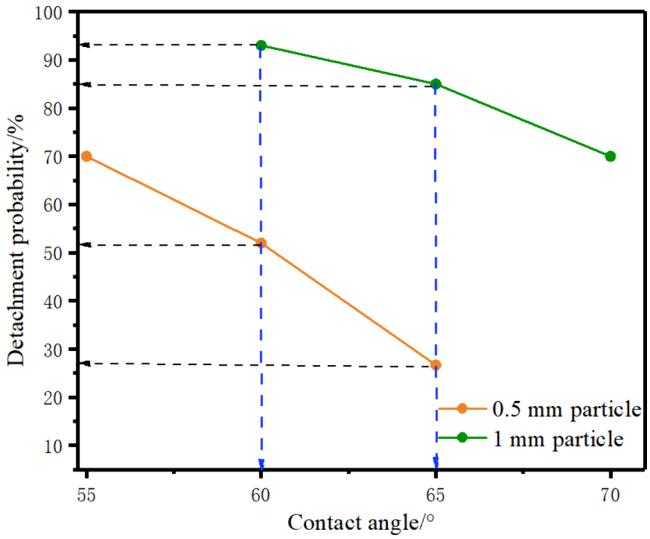

Figure 6. Collision detachment probability of bubble-particle aggregates with various particle sizes and hydrophobicity.

with increasing particle size, but the increased gravity causes the bubble-particle aggregate to become less stable, increasing the detachment probability overall.[28]

3.3. Research on the Collision Detachment Mechanism of Bubble-Particle Aggregates. *3.3.1. Effect of Particle Size on Bubble-Particle Collision Detachment.* A high-speed dynamic camera recorded the bubble-particle collision process, and the detachment behavior of bubble-particle aggregates with varying particle sizes was examined. The collision detachment process of identically hydrophobic 0.5 and 1 mm particles is depicted in Figure 7. It is clear from

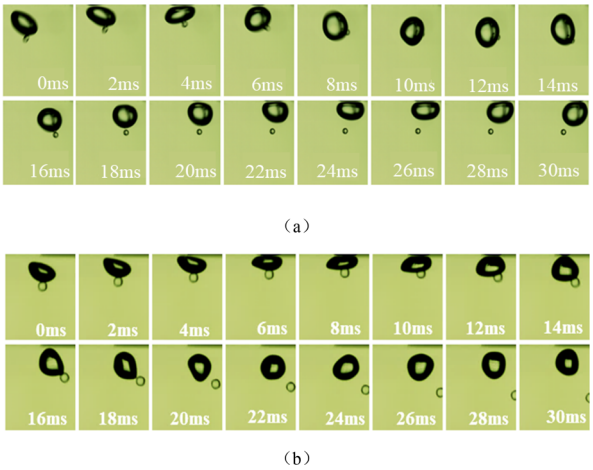

Figure 7. Collision detachment process of bubble-particle aggregates with 0.5 mm particles and 1 mm particles under the same hydrophobicity: (a) 0.5 mm particle and (b) 1 mm particle.

intuition that the two particle sizes exhibit significantly different postcollision deceleration behavior. Following the collision between fine particles and bubbles, the fine particles slide and slow down on the surface of the bubbles while the bubbles slightly deform. Because the larger the particle, the higher its gravity becomes, causing the coarse particles to always dangle below the bubble, the slip degree of the coarse particles on the bubble's surface is significantly decreased. The bubble is compressed by the impact of the vertical collision

https://doi.org/10.1021/acsomega.3c08918
ACS Omega 2024, 9, 4966−4973

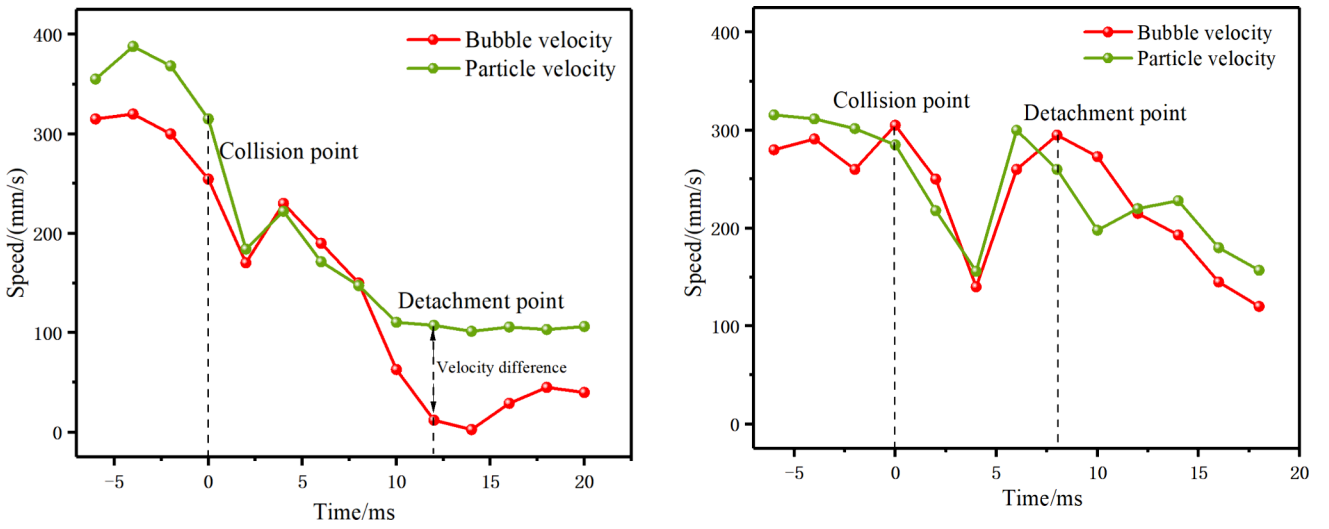

Figure 8. Comparison of particle velocity during collision detachment of bubble-particle aggregates with different particle sizes: (a) 0.5 mm particle and (b) 1 mm particle.

between the particle and the bubble, which significantly raises the bubble's degree of deformation and lowers the coarse particle velocity.[29,30]

To further analyze the effect of particle size on collision detachment, the spatial position coordinates before and after the bubble-particle collision were extracted to study the velocity variation of the bubble-particle aggregates during collision detachment. Figure 8 illustrates the velocity variation curves of various-sized particles and bubbles throughout the collision detachment process. The velocity of fine particles and bubbles continuously drops when the bubble-particle aggregate collides with the substrate with the bubbles decreasing more quickly. When there is the greatest velocity differential between particles and bubbles, detachment takes place. The velocity of coarse particles and bubbles, on the other hand, exhibits the identical pattern of first reducing and then increasing, with no discernible velocity difference during the velocity change process. We infer that the detachment of fine particles, but not of coarse particles, is mostly caused by the velocity differential between particles and bubbles.[31,32]

Additional examination was conducted on the alterations in the bubble projection area of the bubble-particle aggregates, which were created by particles with varying sizes during the collision process, as illustrated in Figure 9. The coarse particle extrusion during collision causes the bubble to shake significantly, as evidenced by the fact that the coarse particle aggregate's variation of bubble area during collision is higher than that of the fine particle aggregate. It is worth noting that the coarser aggregate's bubble area still varies significantly after the collision as compared to fine particles, suggesting that bubble oscillation is the primary driver of coarse bubble-particle aggregate detachment.[33]

3.3.2. Effect of Particle Hydrophobicity on Bubble-Particle Collision Detachment. Analysis was performed on the bubble-particle collision photos under various particle sizes and hydrophobicity. Figure 10 shows the important locations during the collision. The findings indicate that the primary factor influencing the bubble-particle detachment mechanism is the particle size. Particles of the same size but with varying hydrophobicity displayed the same detachment pattern. Bubble oscillation is the main source of 1 mm particle

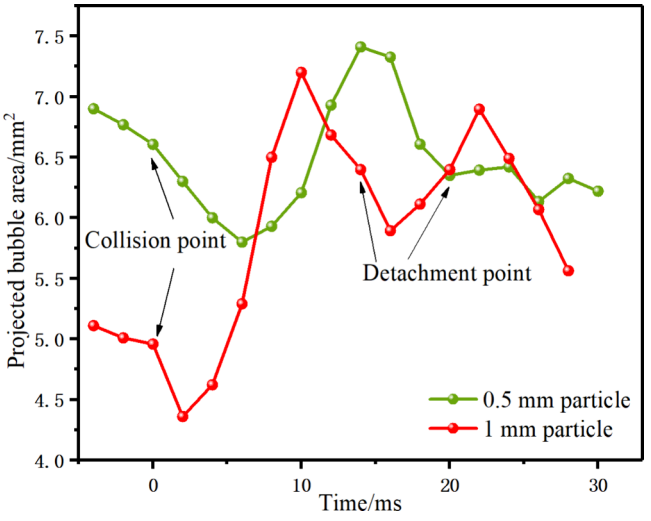

Figure 9. Comparison of projected bubble area during collision detachment of bubble-particle aggregates with different particle sizes.

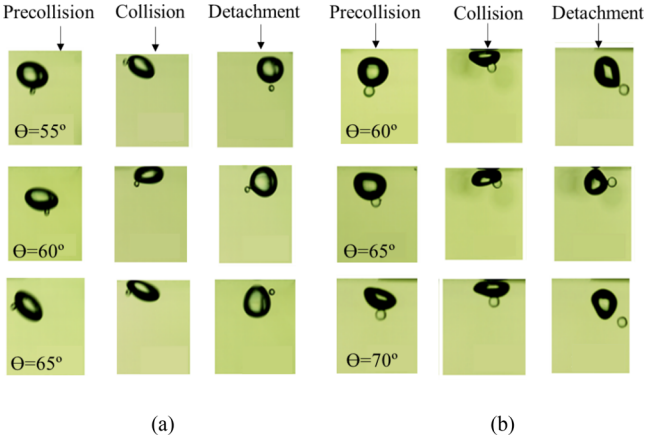

Figure 10. Key images of the bubble-particle collision detachment process under different particle sizes and hydrophobicity: (a) 0.5 mm particle and (b) 1 mm particle.

https://doi.org/10.1021/acsomega.3c08918
ACS Omega 2024, 9, 4966−4973

detachment, while velocity difference is the main cause of 0.5 mm particle detachment.

The particle velocity change curves under various hydrophobicity settings throughout the fine bubble-particle aggregate collision detachment process are depicted in Figure 11. Particle velocity rapidly decreases with time after the bubble-particle aggregate collides with the substrate. For instance, at θ = 55°, there is a duration difference of around 8 ms and a speed difference of approximately 100 mm/s between the collision and detachment points. The duration and velocity difference needed for particle detachment steadily increase with increasing particle hydrophobicity. At θ = 65°, there is a time difference of approximately 26 ms and a velocity differential of approximately 210 mm/s between the collision and detachment points. It is demonstrated that when particle hydrophobicity increases, the stability of the bubble-particle aggregate also increases.

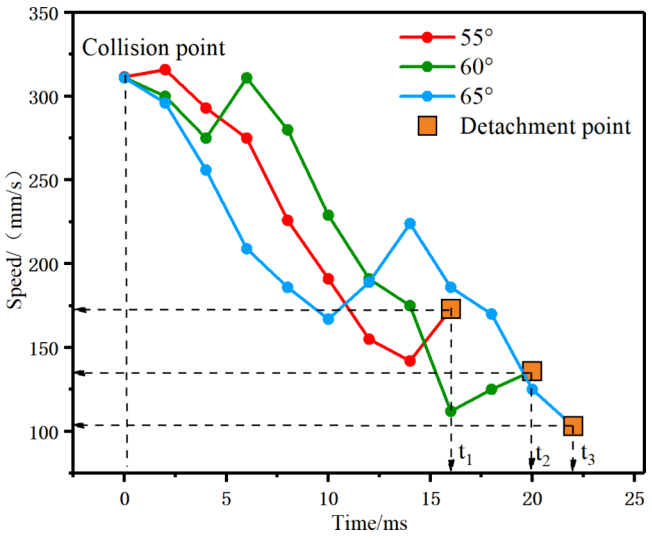

Figure 11. Particle velocity change curves during the detachment process of bubble-particle aggregates with 0.5 mm particles under different hydrophobicity.

Figure 12 shows the change curves of the bubble area during the bubble-particle collision detachment process with 1 mm particles under different hydrophobicity. Time-wise, the projected area of the bubble varies drastically once the bubble-particle aggregate collides with the substrate. After the collision, the bubble area for θ = 60° varies by 0.6 mm^2, with a 14 ms time difference between collision and detachment. Particle detachment increasingly requires more time and area fluctuation as the particle hydrophobicity increases. The area fluctuation of the bubble after collision detachment is in the range of 1.2 mm^2, and the time difference between the collision point and the detachment point is around 28 ms when θ = 70°. It is shown that the stability of bubble-particle aggregates is enhanced with an increase in particle hydrophobicity. This is consistent with the conclusion of bubble-particle collision detachment probability in Section 3.2.

4. CONCLUSIONS

As particle hydrophobicity increases, the probability of detachment of the bubble-particle collision decreases. This is because the interaction force between particles and bubbles increases, enhancing the stability of the bubble-particle aggregates. It has been discovered that particles of different sizes detach due to collision through different mechanisms. When a bubble-particle aggregate collides with the solid surface, the fine particles tend to slide down the bubble's surface due to low gravity. This sliding motion between the particles and the bubbles creates a differential velocity that plays a significant role in the detachment of fine particles. However, the strong gravity of coarse particles can cause bubbles to squeeze vertically and bubble oscillation can contribute to bubble-particle detachment. It was discovered that detachment mode was only related to particle size but not to particle hydrophobicity. Particle hydrophobicity can only increase the stability of the bubble-particle aggregate by gradually increasing the duration and velocity difference needed for the detachment of fine particles and the time and area fluctuation needed for the detachment of coarse particles.

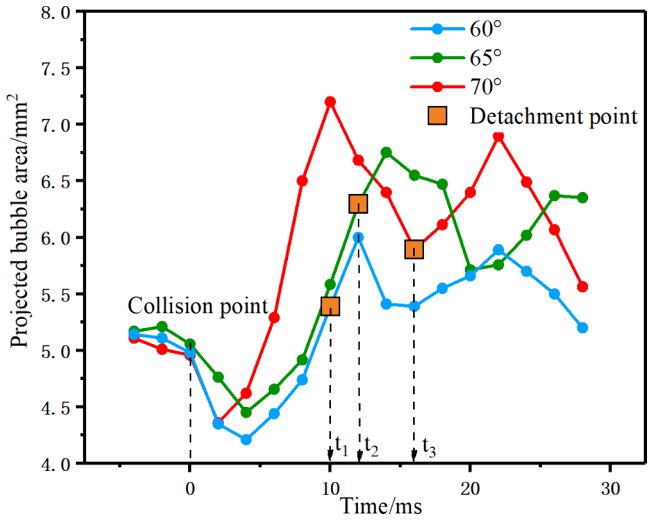

Figure 12. Projected bubble area change curves during the detachment process of bubble-particle aggregates with 1 mm particles under different hydrophobicity.

This paper examines, in a rather ideal setting, the collision detachment behavior of bubble-particle aggregates on solid surfaces, excluding the influence of the foam layer at the slurry−foam phase interface. To investigate the collision detachment behavior of bubble-particle aggregates at the real slurry−foam phase interface, a foam layer coated with bubble-particle aggregates may be added to the test in later research. A 3D detachment model of bubble-particle aggregates can be developed by observing the detachment behavior using several cameras. Real flotation is not limited to bubble-particle aggregates with single particles; in the future, we can investigate the mechanism of particle−particle interaction in bubble-particle aggregates with multiparticles by studying the multiparticle model.

AUTHOR INFORMATION

Corresponding Author

Yaowen Xing − *State Key Laboratory of Coking Coal Resources Green Exploitation, China University of Mining and Technology, Xuzhou 221116, China;* orcid.org/0000-0001-7930-4725; Phone: +86-15062114600; Email: cumtxyw@126.com

https://doi.org/10.1021/acsomega.3c08918
ACS Omega 2024, 9, 4966−4973

Authors

Yiqing Zhang − *State Key Laboratory of Coking Coal Resources Green Exploitation and School of Chemical Engineering and Technology, China University of Mining and Technology, Xuzhou 221116, China;* orcid.org/0009-0007-0908-8685

Shihao Ding − *State Key Laboratory of Coking Coal Resources Green Exploitation and School of Chemical Engineering and Technology, China University of Mining and Technology, Xuzhou 221116, China*

Weihan Si − *State Key Laboratory of Coking Coal Resources Green Exploitation, China University of Mining and Technology, Xuzhou 221116, China*

Qinglin Yin − *State Key Laboratory of Coking Coal Resources Green Exploitation and School of Chemical Engineering and Technology, China University of Mining and Technology, Xuzhou 221116, China*

Chenyimin Yang − *State Key Laboratory of Coking Coal Resources Green Exploitation and School of Chemical Engineering and Technology, China University of Mining and Technology, Xuzhou 221116, China*

Wenqing Shi − *State Key Laboratory of Coking Coal Resources Green Exploitation and School of Chemical Engineering and Technology, China University of Mining and Technology, Xuzhou 221116, China*

Xiahui Gui − *State Key Laboratory of Coking Coal Resources Green Exploitation, China University of Mining and Technology, Xuzhou 221116, China;* orcid.org/0000-0001-9270-7756

Complete contact information is available at: https://pubs.acs.org/10.1021/acsomega.3c08918

Author Contributions

[§]Y.Z. and S.D. contributed equally to this work as co-first authors.

Notes

The authors declare no competing financial interest.

■ ACKNOWLEDGMENTS

This work was supported by the National Nature Science Foundation of China (Nos. 52274278,52174265, and 51920105007).

■ REFERENCES

(1) Xing, Y.; Xu, M.; Gui, X.; Cao, Y.; Babel, B.; Rudolph, M.; Weber, S.; Kappl, M.; Butt, H.-J. The Application of Atomic Force Microscopy in Mineral Flotation. *Adv. Colloid Interface Sci.* **2018**, *256*, 373−392.

(2) Xing, Y.; Gui, X.; Pan, L.; Pinchasik, B.-E.; Cao, Y.; Liu, J.; Kappl, M.; Butt, H.-J. Recent Experimental Advances for Understanding Bubble-Particle Attachment in Flotation. *Adv. Colloid Interface Sci.* **2017**, *246*, 105−132.

(3) Darabi, H.; Koleini, S. M. J.; Deglon, D.; Rezai, B.; Abdollahy, M. Investigation of Bubble-Particle Attachment, Detachment and Collection Efficiencies in a Mechanical Flotation Cell. *Powder Technol.* **2020**, *375*, 109−123.

(4) Hassanzadeh, A.; Safari, M.; Hoang, D. H.; Khoshdast, H.; Albijanic, B.; Kowalczuk, P. B. Technological Assessments on Recent Developments in Fine and Coarse Particle Flotation Systems. *Minerals Engineering* **2022**, *180*, No. 107509.

(5) Liu, J.; Zhang, R.; Bao, X.; Hao, Y.; Gui, X.; Xing, Y. New Insight into the Role of the Emulsified Diesel Droplet Size in Low Rank Coal Flotation. *Fuel* **2023**, *338*, No. 127388.

(6) Feng, D.-X.; Nguyen, A. V. A Novel Quantitative Analysis of the Local Deformation of the Air-Water Surface by a Floating Sphere. *Colloids Surf., A* **2016**, *504*, 407−413.

(7) Feng, D.-X.; Nguyen, A. V. How Does the Gibbs Inequality Condition Affect the Stability and Detachment of Floating Spheres from the Free Surface of Water? *Langmuir* **2016**, *32* (8), 1988−1995.

(8) Feng, D.-X.; Nguyen, A. V. The Floatability of Single Spheres versus Their Pairs on the Water Surface. *Langmuir* **2016**, *32* (51), 13627−13634.

(9) Nutt, C. W. Froth Flotation: The Adhesion of Solid Particles to Flat Interfaces and Bubbles. *Chem. Eng. Sci.* **1960**, *12* (2), 133−141.

(10) Schulz, D.; Reinecke, S. R.; Woschny, N.; Schmidt, E.; Kruggel-Emden, H. Development and Evaluation of Force Balance Based Functions for Dust Detachment from Bulk Particles Stressed by Fluid Flow. *Powder Technol.* **2023**, *417*, No. 118257.

(11) Schulze, H. J. New Theoretical and Experimental Investigations on Stability of Bubble/Particle Aggregates in Flotation: A Theory on the Upper Particle Size of Floatability. *Int. J. Miner. Process.* **1977**, *4* (3), 241−259.

(12) Hanumanth, G. S.; Williams, D. J. A. A Three-Phase Model of Froth Flotation. *Int. J. Miner. Process.* **1992**, *34* (4), 261−273.

(13) Sarhan, A. R.; Homadi, A. M.; Naser, J. Modelling Detachment Rates of Hydrophobic Particles from Bubbles in a Froth Phase. *Sep. Purif. Technol.* **2020**, *235*, No. 116200.

(14) Ata, S. Coalescence of Bubbles Covered by Particles. *Langmuir* **2008**, *24* (12), 6085−6091.

(15) Ata, S. Phenomena in the Froth Phase of Flotation — A Review. *Int. J. Miner. Process.* **2012**, *102*−*103*, 1−12.

(16) Falutsu, M. Column Flotation Froth Characteristics — Stability of the Bubble-Particle System. *Int. J. Miner. Process.* **1994**, *40* (3), 225−243.

(17) Falutsu, M.; Dobby, G. S. Direct Measurement of Froth Drop Back and Collection Zone Recovery in a Laboratory Flotation Column. *Minerals Engineering* **1989**, *2* (3), 377−386.

(18) Seaman, D. R.; Manlapig, E. V.; Franzidis, J.-P. Selective Transport of Attached Particles across the Pulp−Froth Interface. *Minerals Engineering* **2006**, *19* (6), 841−851.

(19) Krasowska, M.; Malysa, K. Kinetics of Bubble Collision and Attachment to Hydrophobic Solids: I. Effect of Surface Roughness. *Int. J. Miner. Process.* **2007**, *81* (4), 205−216.

(20) Ireland, P. M.; Jameson, G. J. Collision of a Rising Bubble−Particle Aggregate with a Gas−Liquid Interface. *Int. J. Miner. Process.* **2014**, *130*, 1−7.

(21) Chipili, C.; Bhondayi, C. The Role of the Water−Air and Pulp-Froth Interfaces on Particle Detachment: Impact of Particle Size, Type, Contact Angle and Bubble Rise Velocity. *Minerals Engineering* **2024**, *205*, No. 108453.

(22) Chipili, C.; Bhondayi, C. The Role of the Pulp-Froth Interface on Particle Detachment and Selectivity. *Adv. Colloid Interface Sci.* **2021**, *287*, No. 102296.

(23) Ding, S.; Yin, Q.; Zhang, Y.; He, Q.; Feng, X.; Yang, C.; Cao, Y.; Gui, X.; Xing, Y. Mechanism of the Hydrophobic Particles with Different Sizes Detaching from the Oscillating Bubble Surface. *Colloids Surf., A* **2022**, *646*, No. 128986.

(24) Zhang, Z.; Zhao, L.; Zhuang, L. Direct Force Measurement of Critical Detachment Force between a Particle and an Air Bubble Using Dynamic Interaction Force Apparatus. *Miner. Eng.* **2020**, *159*, No. 106627.

(25) Feng, D.-X.; Nguyen, A. V. Contact Angle Variation on Single Floating Spheres and Its Impact on the Stability Analysis of Floating Particles. *Colloids Surf., A* **2017**, *520*, 442−447.

(26) Feng, D.-X.; Nguyen, A. V. Effect of Contact Angle and Contact Angle Hysteresis on the Floatability of Spheres at the Air-Water Interface. *Adv. Colloid Interface Sci.* **2017**, *248*, 69−84.

(27) Wang, G.; Nguyen, A. V.; Mitra, S.; Joshi, J. B.; Jameson, G. J.; Evans, G. M. A Review of the Mechanisms and Models of Bubble-Particle Detachment in Froth Flotation. *Sep. Purif. Technol.* **2016**, *170*, 155−172.

(28) Wang, G.; Feng, D.; Nguyen, A.; Evans, G. M. The Dynamic Contact Angle of a Bubble with an Immersed-in-Water Particle and Its Implications for Bubble-Particle Detachment. *Int. J. Miner. Process.* **2016**, *151*, 22−32.
(29) Ngo-Cong, D.; Nguyen, A. V.; Tran-Cong, T. Isotropic Turbulence Surpasses Gravity in Affecting Bubble-Particle Collision Interaction in Flotation. *Minerals Engineering* **2018**, *122*, 165−175.
(30) Hoque, M. M.; Doroodchi, E.; Jameson, G. J.; Evans, G. M.; Mitra, S. Numerical Estimation of Critical Local Energy Dissipation Rate for Particle Detachment from a Bubble-Particle Aggregate Captured within a Confined Vortex. *Minerals Engineering* **2022**, *180*, No. 107508.
(31) Ting, H. Z.; Yang, Y.; Tian, Z. F.; Carageorgos, T.; Bedrikovetsky, P. Detachment of Inclined Spheroidal Particles from Flat Substrates. *Powder Technol.* **2023**, *427*, No. 118754.
(32) Wang, G.; Wang, Y.; Yu, J.; Yao, N.; Zhao, L.; Liu, Y.; Chen, S.; Wang, P. Detachment of a Particle from the Surface of a Bubble Colliding with a Solid Surface. *Powder Technol.* **2023**, *430*, No. 119045.
(33) Zawala, J.; Krasowska, M.; Dabros, T.; Malysa, K. Influence of Bubble Kinetic Energy on Its Bouncing During Collisions with Various Interfaces. *Canadian Journal of Chemical Engineering* **2007**, *85* (5), 669−678.

https://doi.org/10.1021/acsomega.3c08918
ACS Omega 2024, 9, 4966−4973